

# Chiral Selective Transmembrane Transport of Amino Acids through Artificial Channels

Lei Chen,<sup>†</sup> Wen Si,<sup>†</sup> Liang Zhang, Gangfeng Tang, Zhan-Ting Li, and Jun-Li Hou\*

Department of Chemistry, Fudan University, 220 Handan Road, Shanghai 200433, China

**S** Supporting Information

**ABSTRACT:** Peptide-appended pillar[*n*]arene (*n* = 5, 6) derivatives have been synthesized. <sup>1</sup>H NMR and IR studies revealed that the molecules adopt a tubular conformation in solution and lipid bilayer membranes. Kinetic measurements using the fluorescent labeling method with lipid vesicles revealed that these molecules can efficiently mediate the transport of amino acids across lipid membranes at a very low channel-to-lipid ratio (EC<sub>50</sub> = 0.002 mol %). In several cases, chiral selectivity for amino acid enantiomers was achieved, which is one of the key functions of natural amino acid channels.

The transmembrane transport of amino acids, which plays a crucial role in life systems, has been realized by specific transporters,<sup>1</sup> such as the ATP-binding cassette (ABC) superfamily,<sup>2</sup> the phospholemman (PLM) family,<sup>3</sup> and hypotonically activated amino acid channels (HAACs),<sup>4</sup> with high selectivity and efficiency. The development of artificial transporters for amino acids is of importance fundamentally and for practical applications. In recent years, many synthetic systems that can transport various ions,<sup>5</sup> water,<sup>6</sup> and glucose<sup>7</sup> have been described. However, the transport of amino acids by synthetic molecules has been investigated only with simple U-tube experiments across liquid phases.<sup>8</sup> To the best of our knowledge, no examples of amino acid transmembrane transport by synthetic systems have been reported. Because amino acids can pass membranes in the simple diffusion mechanism,<sup>9</sup> the design of any artificial transporters should require an efficiency that is much higher than that of this simple diffusion process. This has been a challenge because for any successful transporter, its concentration should be much lower than that of the transported species. Herein we report that pillar[*n*]arene (*n* = 5, 6) derivatives bearing short peptide chains can serve as efficient artificial channels for transmembrane transport of amino acids that display high chiral selectivity.

We have been interested in the construction of single-molecule artificial transmembrane channels.<sup>10</sup> Previously, we found that hydrazide-appended pillar[5]arenes could form single-molecule tubular structures that are induced by intramolecular N–H···O=C hydrogen bonding of the hydrazide unit.<sup>6c</sup> It was envisioned that peptide-attached pillar[*n*]arenes<sup>11–13</sup> could give rise to similar tubular structures. Thus, a library of pillar[*n*]arene (*n* = 5, 6) amino acid derivatives **1a–c** and **2a–d**, which bear 10 and 12 peptide chains, respectively, with different lengths and sequences were prepared (Figure

1).<sup>14</sup> The nonpolar benzyl group of phenylalanine (Phe) on the peptide chains was expected to increase the membrane-



**1a:** *n* = 5, R = D-Phe-L-Phe-D-Phe-COOH    **2a:** *n* = 6, R = D-Phe-L-Phe-D-Phe-COOH  
**1b:** *n* = 5, R = L-Phe-L-Phe-L-Phe-COOH    **2b:** *n* = 6, R = L-Phe-L-Phe-L-Phe-COOH  
**1c:** *n* = 5, R = L-Phe-D-Phe-L-Phe-COOH    **2c:** *n* = 6, R = L-Phe-COOH  
**3a:** *n* = 5, R = D-Phe-L-Phe-D-Phe-COOEt    **2d:** *n* = 6, R = L-Phe-L-Phe-COOH  
**3b:** *n* = 5, R = L-Phe-L-Phe-L-Phe-COOEt

**Figure 1.** Structures of compounds **1a–c**, **2a–d**, **3a**, and **3b**.

insertion ability of the molecules. Both D- and L-Phe were used to build the peptide chains to produce channels with different chiral cavities.

The possibility of forming intramolecular hydrogen bonds in bulk and lipid bilayer membranes was first investigated by using as model compounds **3a** and **1a** (Figure 1), respectively, which have the same main scaffold. In CD<sub>2</sub>Cl<sub>2</sub>, **3a** produced a <sup>1</sup>H NMR spectrum of high resolution with the signals of the three amide protons (from inside to outside) located at 7.67, 6.99, and 7.62 ppm, respectively, as assigned by two-dimensional (2D) correlation spectroscopy (COSY) and rotating-frame Overhauser effect spectroscopy (ROESY) experiments [Figures S51–S56 in the Supporting Information (SI)]. These signals were shifted downfield significantly (0.7–1.3 ppm) relative to the related signals of control **4** (Figure 2a,b). Diluting the solution from 5 to 0.2 mM did not cause an observable shift in the N–H signals. These results suggested that the peptide chains of **3a** engage in intramolecular hydrogen bonding, which should induce the whole peptide chains to form a tubular structure (Figure 2c and Figure S57).<sup>6c</sup> For further investigation of the structure in the lipid phase, **1a** and **5** were inserted into the membranes of large unilamellar vesicles (LUVs) made from egg yolk L- $\alpha$ -phosphatidylcholine (EYPC). Relative to that of C=O(NH) of **5** at 1645 cm<sup>-1</sup>, the IR stretch band of **1a** shifted to 1660 cm<sup>-1</sup> (Figure S58), suggesting that **1a** also assembles into a tubular structure in lipid membranes.<sup>15</sup> <sup>1</sup>H NMR and IR experiments for **1b** and **3b**

**Received:** December 31, 2012

**Published:** January 30, 2013

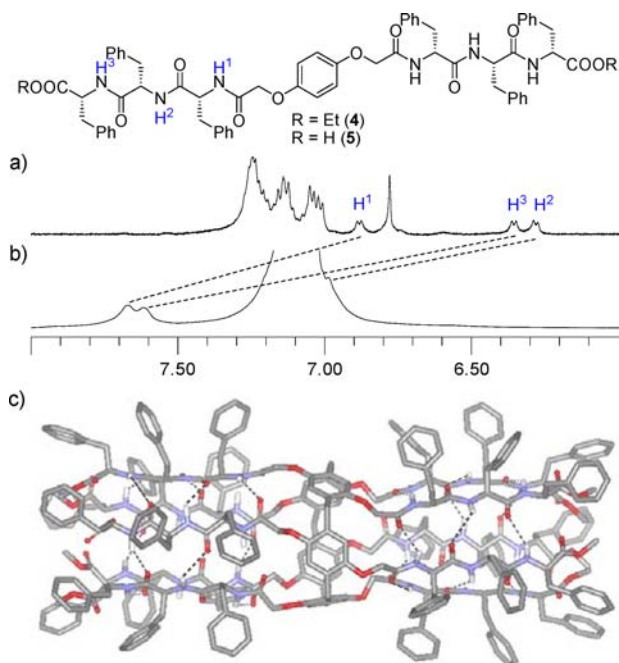


**Figure 2.** (a, b) Partial <sup>1</sup>H NMR spectra of (a) **4** (25 mM) and (b) **3a** (5.0 mM) in CD<sub>2</sub>Cl<sub>2</sub> at 298 K. (c) Molecular modeling (Gaussian 09, semiempirical, PM6) structure of **3a** (H atoms on the C atoms have been omitted for clarity).

revealed similar results, indicating that these two compounds form similar tubular structures. Since the peptide chains of **2a** and **2b** possess the same arrangement as in **1a** and **1b**, it is rational to assume that their peptide chains also form similar tubular conformations in lipid membranes.

The potential of the tubular molecules for transport of Gly was then explored first by using <sup>13</sup>C NMR experiments.<sup>16</sup> The LUV solution was prepared in HEPES-buffered D<sub>2</sub>O (pD 6.5), and then 1-<sup>13</sup>C-labeled Gly (Gly-1-<sup>13</sup>C, 150 mM) and the chemical shift reagent EuCl<sub>3</sub> (300 mM) were added. In the presence of **1b** [molar ratio relative to lipid ( $x$ ) = 0.05%, corresponding to 170 molecules of **1b** per vesicle<sup>17</sup>], trans-membrane transport of Gly was observed over the course of 80 min, as reflected by the appearance of a small peak at 171.7 ppm corresponding to the O=C<sup>13</sup>C signal of Gly loaded in the vesicles (Figure 3). However, in the absence of **1b**, only very

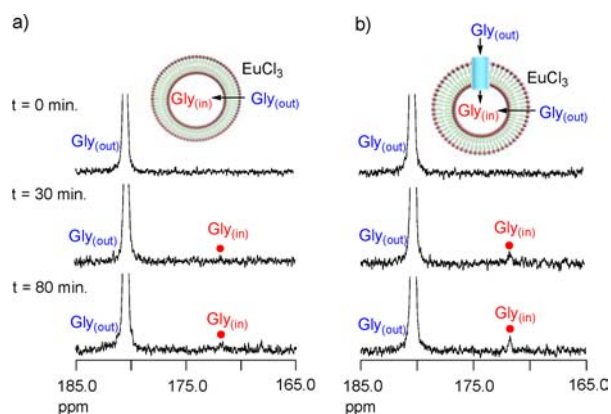


**Figure 3.** Partial <sup>13</sup>C NMR spectra indicating the transport of Gly-1-<sup>13</sup>C cross the lipid membrane in the (a) absence and (b) presence of **1b** ( $x = 0.05\%$ ).

slow transport of Gly was detected. Cryogenic transmission electron microscopy (cryo-TEM) showed that in the presence of **1b** ( $x = 0.05\%$ ), the vesicles did not break over the course of 3 h (Figure S59), indicating that the vesicles were stable after incorporation of **1b** into their membranes. Thus, the increased transport efficiency in the presence of **1b** should be attributed to the channel created by its tubular structure formed in the membranes.

The transport kinetics was measured quantitatively using the fluorescent labeling method.<sup>9a</sup> Thus, LUVs containing Gly (13 mM) were first prepared in HEPES buffer (pH 7.0) and put into a dialysis tube immersed in the same buffer. Next, a DMSO solution of **1b**, **2b**, **2c**, or **2d** ( $x = 0.05\%$ ) was injected into the vesicle solution. Aliquots of the solution outside the dialysis tube were taken out and then treated with fluorescent probe fluorescamine.<sup>18</sup> In this way, the Gly transported from the inside of the vesicles was labeled with the probe by formation of a lactam. By measuring the fluorescent intensity, the Gly concentrations ([Gly]) were determined. Plots of [Gly] against time are shown in Figure 4. For the systems containing **1b** and

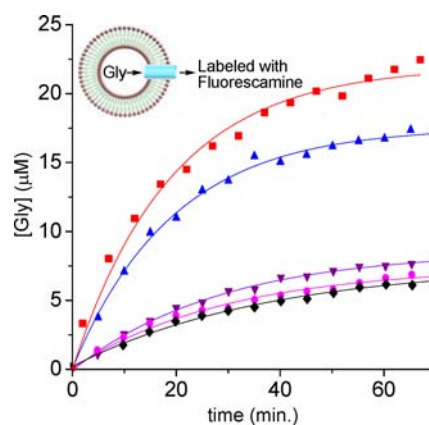


**Figure 4.** Gly concentration outside the vesicles vs time after addition of pure DMSO (♦) or a solution of **1b** (▲), **2b** (■), **2c** (●), or **2d** (▼) ( $x = 0.05\%$ ) in DMSO. Inset: schematic representation of the transport process.

**2b**, [Gly] increased dramatically from 0 to 20 and 23 μM, respectively, in 70 min, whereas for the systems containing the shorter molecules **2c** and **2d**, the concentration increased to only 6 and 7 μM, respectively. In the absence of tubular compounds, the concentration increase was 5 μM. From fits of the data using a nonlinear model,<sup>9a</sup> the Gly transport rate constants ( $k$ ) for **1b**, **2b**, **2c**, and **2d** were calculated to be  $(8.7 \pm 0.1) \times 10^{-4}$ ,  $(9.0 \pm 0.2) \times 10^{-4}$ ,  $(3.0 \pm 0.1) \times 10^{-4}$ , and  $(4.2 \pm 0.1) \times 10^{-4} \text{ s}^{-1}$ , respectively. The transport rate constant in the absence of channels, ( $k_0$ ) was determined to be  $(2.7 \pm 0.1) \times 10^{-4} \text{ s}^{-1}$ , indicating that Gly was transported across the lipid membrane without channels, but slowly.<sup>9a</sup> In view of the very low  $x$  value, the efficiency of the transport by **1b** and **2b** was actually much higher than that of simple diffusion. The fact that **2b** displayed a higher transport rate than **2c** and **2d** might be rationalized by considering that the length of its hydrophobic part (3.2 nm as estimated using a CPK model) better matched the width of the hydrophobic part of the lipid membrane (3.5 nm).<sup>5b</sup>

Transport rates at different channel concentrations were also measured for **1b**. It was found that the transport activity ( $A \equiv k/k_0$ ) was strongly dependent on  $x$ . As  $x$  increased from 0 to

0.05%,  $A$  increased significantly. Further increasing  $x$  caused only a slight increase in  $A$  (Figure S60). The effective concentration needed for 50% activity ( $EC_{50}$ ) and the Hill coefficient ( $n$ ) were calculated to be 0.002% and 0.7,<sup>19</sup> respectively (Figure S61). Such a low  $EC_{50}$  compared with those of other artificial transporters of ions,<sup>20</sup> water,<sup>6c</sup> and glucose<sup>7</sup> indicates that the new tubular channel is very effective in transporting Gly, while the small  $n$  value shows that it works in a single-molecule manner.<sup>19,21</sup>

The abilities of **1a**, **1b**, **2a**, and **2b** to transport other natural amino acids, including Ala, Ser, Thr, Val, Leu, and Phe, were also investigated using the same method (Figures S62–S68) and were found to decrease in the order Gly > Ala > Ser > Thr > Val > Leu > Phe, which is consistent with the increasing size of the amino acids (Figure 5). For the same small amino acids

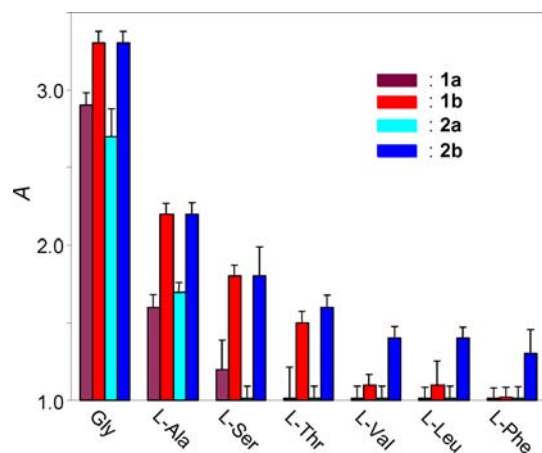


**Figure 5.** Transport activities ( $A$ ) of the channels **1a**, **1b**, **2a**, and **2b** ( $x = 0.05\%$ ) for different natural amino acids ( $A = 1.0$  indicates no transport activity).

(Gly, Ala, and Ser), **1b** and **2b** showed very similar transport activities. For the other larger amino acids, the transport activity of **1b** was decreased gradually in the order Thr > Val > Leu > Phe, reflecting the increasing amino acid size. The transport activity of **2b** for these larger amino acids also decreased with increasing amino acid size but was generally higher than that of **1b**, which might be attributed to the larger cavity of **2b**.<sup>22</sup> Channels **1a** and **2a** transported only the smallest amino acids, Gly and Ala (Figure 5). This result shows that the selectivity of this kind of tubular channel for different amino acids can be tuned simply by changing the sequence of the attached peptide chains.

Because the tubular molecules bear chiral peptide chains, we also investigated their capacity to discriminate enantiomers of chiral Ala, Ser, Thr, Val, Leu, and Phe. It was revealed that channel **2b** could mediate the transport of all enantiomers of the first five amino acids (Figure 6a). However, transport of the D isomer was faster than that of the L isomer in every case, and this difference increased with increasing amino acid size. For Phe, only transport of the L isomer could be mediated (Figure 6a,b). Similar selective transport of D-Leu by **1a**, **1b**, and **2a** and D-Ser by **2a** could also be realized (Table S2 in the SI). For other amino acids, these channels transported both isomers with an efficiency that depended on the structure of the amino acid (Table S2). The observed high selectivity indicates that the difference in the binding between the chiral amino acids and the chiral environment formed by the peptide chains might be

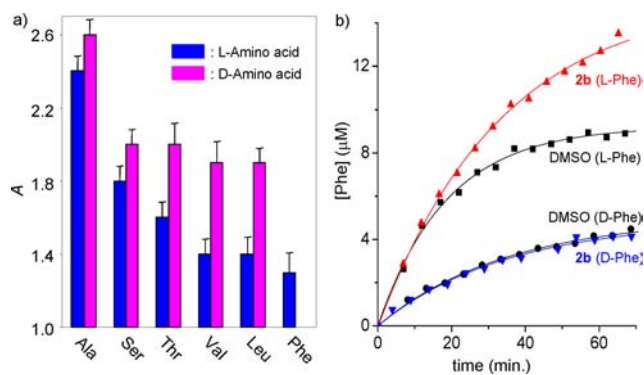


**Figure 6.** (a) Transport activities ( $A$ ) of **2b** ( $x = 0.05\%$ ) for L- and D-amino acids. (b) Changes in L- or D-Phe concentration ( $[Phe]$ ) outside the vesicles with time in the absence or presence of channel **2b** ( $x = 0.05\%$ ).

large enough to make the unfavorable transport negligible compared with the “background” diffusion. Transport of the two isomers of Phe by **1c**, the enantiomer of **1a**, was also investigated and found to favor D-Phe.

It has been reported that natural transporters (e.g., solute carrier families) carry amino acids but block  $Cl^-$ ,<sup>23</sup> whereas some other transporters (e.g., PLM and HAAC systems<sup>1a</sup>) allow the transport of both species. The  $Cl^-$  transport behavior of the new artificial channels was then also studied using the reported method.<sup>20</sup> Thus, a solution of vesicles entrapping the  $Cl^-$ -sensitive dye lucigenin was added to a buffer containing NaCl to produce a NaCl gradient. The flux of NaCl through the channels into the vesicles was assessed by monitoring the fluorescence intensity of lucigenin. Upon addition of **1a**, **1b**, **2a**, or **2b** ( $x = 0.05\%$ ) to the above vesicle solution, the fluorescence intensity increased significantly, reaching 91, 87, 99, and 52%, respectively, after 12 min (Figure 7a). This result demonstrates that the channels are also capable of transporting  $Cl^-$ .<sup>20</sup> When the vesicles contained Gly (10 mM), which was shown by the above fluorescence experiments to pass the

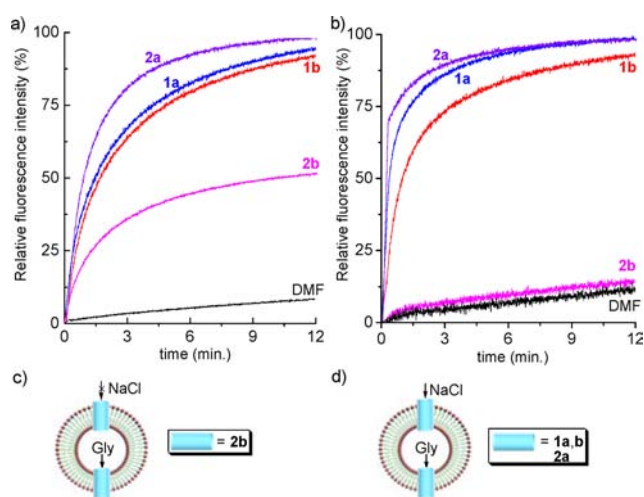


**Figure 7.** (a, b) Changes in fluorescence intensity ( $\lambda_{ex} = 372$  nm,  $\lambda_{em} = 503$  nm) with time after addition of **1a**, **1b**, **2a**, or **2b** ( $x = 0.05\%$ ) to vesicles (a) not containing or (b) containing Gly (10 mM). (c, d) Schematic representations of (c)  $Cl^-$  transport suppression for **2b** and (d) independent  $Cl^-$  transport for **1a**, **1b**, and **2a** in the presence of Gly.

channels much quicker than the other amino acids (Figure 5), the fluorescence enhancement of the **1a**, **1b**, and **2a** systems changed slightly (Figure 7b). However, for the **2b** system, this fluorescence enhancement was weakened remarkably (Figure 7b), indicating that the transport of Cl<sup>-</sup> by **2b** was suppressed considerably (Figure 7c). Fluorescent labeling experiments showed that the transport of Gly by the four channels was not affected by the presence of Cl<sup>-</sup> outside the vesicles.

The fact that Gly and Cl<sup>-</sup> did not affect each other with respect to transport by **1a**, **1b**, and **2a** (Figure 7d) might be rationalized by the following considerations. The amount of channel was much lower than that of lipid, meaning that there was only a small chance for Gly or Cl<sup>-</sup> to approach an inserted channel simultaneously. As a result, the apparent occupancy of the inserted channels by either of them was low, so transport of one did not suppress transport of the other. The transport of Cl<sup>-</sup> by **2b** was notably lower than that by **1a**, **1b**, and **2a**, while the transport of Gly by all of them was comparable. We might propose that binding of Cl<sup>-</sup> to the inserted **2b** is weaker, thus increasing the probability of its transport being blocked by Gly.

In conclusion, we have developed a class of artificial transmembrane amino acid channels from peptide-appended pillar[*n*]arenes (*n* = 5, 6). The whole molecules are induced to form a tubular architecture by the intramolecular hydrogen bonding of the peptide chains. This unique shape enables efficient transport of amino acids across membranes in a single-molecule manner. In several cases, chiral selectivity was realized, which is one of the key functions of natural amino acid channels.<sup>1a</sup> Because the new single-molecule channels possess relatively fixed diameters, we envision that they may also mediate the transmembrane transport of longer peptides consisting of the studied amino acids, which is currently being investigated.

## ■ ASSOCIATED CONTENT

### Supporting Information

Synthetic procedures and characterization data for **1–5**; IR and 2D <sup>1</sup>H NMR spectra and cryo-TEM images; and detailed procedures and measurement data for amino acid and Cl<sup>-</sup> transport. This material is available free of charge via the Internet at <http://pubs.acs.org>.

## ■ AUTHOR INFORMATION

### Corresponding Author

houjil@fudan.edu.cn

### Author Contributions

<sup>†</sup>L.C. and W.S. contributed equally.

### Notes

The authors declare no competing financial interest.

## ■ ACKNOWLEDGMENTS

This work was supported by NSFC (20902012 and 91027008), FANEDD (200930), and the Program for Changjiang Scholars and Innovative Research Team in University (IRT1117).

## ■ REFERENCES

- (1) (a) Saier, M. H., Jr. *Microbiology* **2000**, *146*, 1775. (b) Bröer, S. *Physiol. Rev.* **2008**, *88*, 249.
- (2) Saurin, W.; Hofnung, M.; Dassa, E. *J. Mol. Evol.* **1999**, *48*, 22.
- (3) Chen, L. S. K.; Lo, C. F.; Numann, R.; Cuddy, M. *Genomics* **1997**, *41*, 435.
- (4) Vieira, L. L.; Lafuente, E.; Gamarro, F.; Cabantchik, Z. I. *Biochem. J.* **1996**, *319*, 691.

- (5) (a) Akerfeldt, K. S.; Lear, J. D.; Wasserman, Z. R.; Chung, L. A.; DeGrado, W. F. *Acc. Chem. Res.* **1993**, *26*, 191. (b) Gokel, G. W.; Mukhopadhyay, A. *Chem. Soc. Rev.* **2001**, *30*, 274. (c) Fyles, T. M. *Chem. Soc. Rev.* **2007**, *36*, 335. (d) Davis, A. P.; Sheppard, D. N.; Smith, B. D. *Chem. Soc. Rev.* **2007**, *36*, 348. (e) Li, X.; Wu, Y.-D.; Yang, D. *Acc. Chem. Res.* **2008**, *41*, 1428. (f) Matile, S.; Vargas Jentzsch, A.; Montenegro, J.; Fin, A. *Chem. Soc. Rev.* **2011**, *40*, 2453. (g) Gale, P. A. *Acc. Chem. Res.* **2011**, *44*, 216.

- (6) (a) Percec, V.; Dulcey, A. E.; Balagurusamy, V. S. K.; Miura, Y.; Smirdrcal, J.; Peterca, M.; Numellin, S.; Edlund, U.; Hudson, S. D.; Heiney, P. A.; Duan, H.; Magonov, S. N.; Vinogradov, S. A. *Nature* **2004**, *430*, 764. (b) Duc, Y. L.; Michau, M.; Gilles, A.; Gence, V.; Legrand, Y.-M.; Lee, A.; Tingry, S.; Barboiu, M. *Angew. Chem., Int. Ed.* **2011**, *50*, 11366. (c) Hu, X.-B.; Chen, Z.; Tang, G.; Hou, J.-L.; Li, Z.-T. *J. Am. Chem. Soc.* **2012**, *134*, 8384.

- (7) (a) Cho, H.; Widanapathirana, L.; Zhao, Y. *J. Am. Chem. Soc.* **2011**, *133*, 141. (b) Cho, H.; Zhao, Y. *Langmuir* **2011**, *27*, 4936. (c) Zhang, S.; Zhao, Y. *Chem.—Eur. J.* **2011**, *17*, 12444.

- (8) For examples, see: (a) Demirel, N.; Bulut, Y.; Hosgoren, H. *Tetrahedron: Asymmetry* **2004**, *15*, 2045. (b) Bozkurt, S.; Yilmaz, M.; Sirit, A. *Chirality* **2012**, *24*, 129.

- (9) (a) Chakrabarti, A. C.; Deamer, D. W. *Biochim. Biophys. Acta* **1992**, *1111*, 171. (b) Chakrabarti, A. C. *Amino Acids* **1994**, *6*, 213.

- (10) Si, W.; Chen, L.; Hu, X.-B.; Tang, G.; Chen, Z.; Hou, J.-L.; Li, Z.-T. *Angew. Chem., Int. Ed.* **2011**, *50*, 12564.

- (11) (a) Ogoshi, T.; Kanai, S.; Fujinami, S.; Yamagishi, T.-A.; Nakamoto, Y. *J. Am. Chem. Soc.* **2008**, *130*, 5022. (b) Li, C.; Xu, Q.; Li, J.; Yao, F.; Jia, X. *Org. Biomol. Chem.* **2010**, *8*, 1568. (c) Cragg, P. J.; Sharma, K. *Chem. Soc. Rev.* **2012**, *41*, 597. (d) Xue, M.; Yang, Y.; Chi, X.; Zhang, Z.; Huang, F. *Acc. Chem. Res.* **2012**, *45*, 1294.

- (12) Hu, X.-B.; Chen, L.; Si, W.; Yu, Y.; Hou, J.-L. *Chem. Commun.* **2011**, *47*, 4694.

- (13) Yu, G.; Xue, M.; Zhang, Z.; Li, J.; Han, C.; Huang, F. *J. Am. Chem. Soc.* **2012**, *134*, 13248.

- (14) Theoretically, **1a**, **1b**, **2a**, and **2b** could exist as diastereomers. However, their <sup>1</sup>H NMR spectra displayed one set of signals of high resolution. This result indicates that only one of the diastereomers was formed for each of the compounds, although we do not know its absolute configuration.

- (15) Ghadiri, M. R.; Granja, J. R.; Buehler, L. K. *Nature* **1994**, *369*, 301.

- (16) Davis, J. T.; Gale, P. A.; Okunola, O. A.; Prados, P.; Iglesias-Sánchez, J. C.; Torroba, T.; Quesada, R. *Nat. Chem.* **2009**, *1*, 138.

- (17) Mimms, L. T.; Zampighi, G.; Nozaki, Y.; Tanford, C.; Reynolds, J. A. *Biochemistry* **1981**, *20*, 833.

- (18) Udenfriend, S.; Stein, S.; Böhlen, P.; Dairman, W.; Leimgruber, W.; Weigle, M. *Science* **1972**, *178*, 871.

- (19) Matile, S.; Sakai, N.; Hennig, A. Transport Experiments in Membranes. In *Supramolecular Chemistry: From Molecules to Nanomaterials*; Gale, P. A., Steed, J. W., Eds.; Wiley: Chichester, U.K., 2012; Vol. 2, p 473 ff.

- (20) Busschaert, N.; Wenzel, M.; Light, M. E.; Iglesias-Hernandez, P.; Perez-Tomas, R.; Gale, P. A. *J. Am. Chem. Soc.* **2011**, *133*, 14136.

- (21) Bhosale, S.; Matile, S. *Chirality* **2006**, *18*, 849.

- (22) Han, C.; Ma, F.; Zhang, Z.; Xia, B.; Yu, Y.; Huang, F. *Org. Lett.* **2010**, *12*, 4360.

- (23) Carpenter, V. K.; Drake, L. L.; Aguirre, S. E.; Price, D. P.; Rodriguez, S. D.; Hansen, I. A. *J. Insect Physiol.* **2012**, *58*, 513.